Journal of the Iranian Chemical Society
https://doi.org/10.1007/s13738-017-1262-2

ORIGINAL PAPER

Virtual screening of some heterocyclic structures toward novel antibacterial agents

Zahra S. Hosseini[1] · Mohammad Reza Housaindokht[1] · Nima Razzaghi-Asl[2] · Ramin Miri[3]

Received: 30 April 2017 / Accepted: 30 November 2017

Abstract
Infectious diseases and their treatment are among the most important issues in global health and economy. Moreover, increasing prevalence of antibiotic-resistant pathogenic bacteria necessitates the considerable need for discovering new drugs. Some heterocyclic structures with dihydropyridine (DHP) scaffold have been reported as antimicrobial agents. Herein, we report a structure-based virtual screening of a pool of 3,5-disubstituted DHPs and a post-analysis of virtual hits through in vitro antibacterial assessment. Four top-ranked DHP structures (**6a**–**d**) were found to interact with the relevant target active sites and exhibited superior stereoelectronic features within their enzyme inhibition. Selected compounds were synthesized and assessed for their antibacterial activity via microdilution method. Results of this study represented a significant application of multi-step virtual screening strategy in identifying privileged DHP structures as good starting points for further developments toward more potent antibacterial agents.

Keywords Antibiotic resistance · Dihydropyridine · Docking · Virtual screening · In vitro

Introduction

The remarkable role of bacterial infections in mortality has become a big concern and human life has been always associated with risks related to such infectious diseases. During the past century, many prosperous efforts have been performed to control infectious diseases, but the prevention and treatment of infectious diseases still remained a serious problem in public health, leading to over 13 million deaths each year [1]. Within antimicrobial therapy, antibiotic resistance is one of the major challenges and is usually considered to be a consequence of antibiotic misuse. Nowadays, many of bacteria are resistant to at least one of the most commonly used drugs. Therefore, existing drugs can't properly respond to the control and treatment of many infectious diseases, and hence, design and development of new and more effective antibacterial agents are an urgent requirement in human life [2].

Considerable advances in the field of computational chemistry and protein crystallography facilitated most of the traditional efforts toward discovery of novel chemotherapeutic agents [3]. In silico or computer-aided drug design is a rational drug discovery technique that serves as a fundamental part of modern drug discovery projects. In this regard, one of the most efficient strategies is virtual screening (VS) of chemical databases with the aim of finding novel bioactive compounds [4]. Virtual screening tries to efficiently reduce the defined chemical space to a much smaller subset that can be synthesized and assessed through biological targets with the aim of achieving potential lead/drug candidates. It has been postulated that VS can reduce costs and increase hit rates in a typical lead discovery path [5] and therefore may be an alternative approach to high-throughput screening (HTS) [6].

Structure-based virtual screening (SBVS) utilizes docking algorithms to explore the conformational space of ligand–receptor complex [7]. The outputs are top-ranked

Electronic supplementary material The online version of this article (https://doi.org/10.1007/s13738-017-1262-2) contains supplementary material, which is available to authorized users.

✉ Mohammad Reza Housaindokht
housain@um.ac.ir

[1] Department of Chemistry, Faculty of Sciences, Ferdowsi University of Mashhad, Mashhad 9177948974, Iran

[2] Department of Medicinal Chemistry, School of Pharmacy, Ardabil University of Medical Sciences, Ardabil, Iran

[3] Medicinal and Natural Products Chemistry Research Center, Shiraz University of Medical Sciences, Shiraz, Iran

Published online: 04 December 2017

ligand conformations that represent the probable binding modes in the active site of the macromolecular target. SBVS methods require the information of the 3D structure of a target obtained from X-ray crystallography or nuclear magnetic resonance spectroscopy. Such information can be retrieved form a protein data bank (PDB; http://www.rcsb.org) or homology modeled from a homologous protein possessing close sequence identity and order [8].

Several VS strategies have been successfully applied to identify novel antibacterial compounds [9–11]. In the present contribution, a pool of DHP compounds was subjected to SBVS technique with the aim of finding new antibacterial agents. Besides calcium channel blocking activity which is the major biological effect of DHP compounds, there are several other effects such as *p*-glycoprotein inhibition [12], cyclooxygenase-2 inhibition [13], antituberculosis [14] and anticonvulsant [15].

1,4-Dihydropyridine compounds with 3 and 5*N*-naphthyl amide substituents exhibited higher inhibitory effect on *S. aureus* and *E. coli* with regard to methyl ester containing derivatives [16]. It was also revealed that within *N*-naphthyl compounds, 4-chloro phenyl moiety in the C4 of DHP ring produced compounds with higher activity against *S. aureus* than ciprofloxacin [16]. In *N*-benzothiazolyl DHPs, 3,5-estric derivatives showed better activity profile than 3,5-diketone derivatives against *S. aureus* [17]. In a research on 3,5-bis amide derivatives, it was observed that incorporation of *N*-(3,4-dichlorophenyl) and *N*-(2,4,5-tri chlorophenyl) rings into the nitrogen of amide group led to the increase in antibacterial effect against cloxacillin-resistant *S. aureus* [18].

In the light of above explanations and with the aim of developing DHP-based antibacterial compounds and also to further extend the scope of DHP derivatives as privileged biological structures, structures with nitrogen/sulfur heterocycles within the amide substituents and also phenyl derivatives on the C4 of the ring were considered for this study. We report the identification of a few antibacterial compounds. For this purpose, multi-step VS of a collection of 3,5-bis-*N*-aryl carbonylated-4-aryl-1,4-dihydropyridine structures followed by synthesis, characterization and in vitro antibacterial assessment was performed.

Experimental

Ligand dataset

A chemical collection including about 1000 diverse 3,5-bis-carbamoylated 1,4-dihydropyridine structures was designed and prepared electronically (Supplementary file 1). Chemical moieties incorporated into the carbamoyl groups of the DHP structures included phenyl or substituted phenyl derivatives, while aryl or 5/6-membered heteroaryl rings were substituted on the C4 position of the DHP core. All of the 3D structures were subjected to geometric optimization using semi-empirical PM3 method.

Structure-based virtual screening (SBVS)

SBVS was carried out using automated flexible ligand module of the advanced program AutoDock 4.2 [19]. The high-resolution crystal structures of selective therapeutic targets from selected pathogenic bacteria *E. coli* (PDB ID **3FV5**) and *S. aureus* (PDB ID **1SFJ**) were obtained from the Brookhaven Protein Data Bank (RCSB) (http://www.rcsb.org). Before docking the ligands into the macromolecular active sites, the enzymes were processed by removal of the substrate cofactor as well as cognate ligands along with all crystallographic water molecules. All the missing residues were reconstructed through the "check for missing atoms" and "repair missing atoms" module incorporated into the Misc module of the AutoDock tools environment.

2D schematic representations of ligand–enzyme interactions were all reproduced by Ligplot program [20].

The interaction/binding between DHPs and target enzyme active site were modeled using Lamarckian genetic algorithm (LGA). Fifty independent GA runs were performed for each ligand under study. For Lamarckian GA, 27,000 maximum generations, a gene mutation rate of 0.02, and a crossover rate of 0.8 were used. The grid maps of docking studies were generated by AutoGrid program. The size of grid was set in a way to include only the active site but also considerable portions. For this purpose, the *x*, *y*, *z*-coordinates of the grid were set to $60 \times 60 \times 60$ Å^3 around the mass centers of the cognate ligands as the catalytic site of enzyme (spacing 0.375 Å). Cluster analysis was performed on the docked results using an RMSD tolerance of 2 Å.

Filtration criteria

A variety of filtration criteria including estimated binding affinity within multiple target conformations, conformational population of top-ranked cluster and chemical interactions with the key residues of the macromolecular active sites were considered to filter the candidates and hence pick up the molecules that might hit the target successfully. It should be notified that crystal structures from bacteria *E. coli* (PDB ID **3FV5**) and *S. aureus* (PDBID **1SFJ**) were utilized to run the SBVS project and primary hit candidates were selected on the basis of predicted binding affinities within these crystallographic systems.

Chemistry

All of the reagents for the synthesis were obtained from Merck Chemical Company and used without further purification. Melting points were recorded by a Reichert–Jung hot-stage microscope and were uncorrected. ^{1}H NMR spectra were determined on a Bruker FT-500 MHz spectrometer in chloroform-d_1 or DMSO-d_6 depended on the solubility of samples (Supplementary file 2). All the chemical shifts were reported as (δ) values (ppm) against tetramethylsilane as an internal standard. FT-IR (KBr) spectra were determined by a Nicolet FT-IR Magna 550 spectrophotometer.

The analytical thin-layer chromatography (TLC) on precoated silica gel 60 F254 aluminum plates (Merck, Germany) was applied to check the progress of the reactions and purity of the products. Preparative thin-layer chromatography was performed with prepared glass-backed plates (20 × 20 cm^2, 500 µ) using silica gel (Merk Kieselgel 60 HF254, Art. 7739).

General procedure for the synthesis of *N*-aryl-3-oxobutanamides (3a and 3b)

N-Aryl-3-oxobutanamides (***3a*** and ***3b***) were synthesized according to the modified method of Clemens via condensation of 2,2,6-trimethyl-1,3-dioxine-4-one (**1**) and corresponding arylamines (**2a** and **2b**) [21].

N-(2-Benzothiazolyl)-3-oxobutanamide (3a)

Pale yellow crystals; Yield 65%; m.p. 214–216 °C; ^{1}H NMR (DMSO-d_6) d (ppm) 11.65 (brs, 1H, NH-amide), 7.86 (d, J = 7.6 Hz, 1H, C4′-H benzothiazole), 7.68 (d, J = 8.0 Hz, 1H, C7-H benzothiazole), 7.35 (t, J = 8.4 Hz, 1H, C5′-H benzothiazole), 7.20 (t, J = 8.0 Hz, 1H, C6′-H benzothiazole), 3.73 (s, 2H, $COCH_2CO$), 2.23 (s, 3H, CH_3CO); IR (KBr) ν (cm^{-1}): 3178.7 (N–H, amide), 3067.5 (C–H, aromatic), 2917.3 and 2859.2 (C–H, aliphatic), 1719.4 (C=O, ketone), 1661.3 (C=O, amide).

N-(4-Methyl-2-benzothiazolyl)-3-oxobutanamide (3b)

Pale yellow precipitate; Yield 80%; m.p. 158–160 °C; ^{1}H NMR (DMSO-d_6): δ (ppm) 12.48 (NH-amide, s, 1H), 7.14–7.85 (ArH, m, 3H), 3.73 ($COCH_2CO$, s, 2H), 2.20 (CH_3CO, s, 3H), 2.54 (C4′-CH_3-benzothiazol, s, 3H); IR (KBr) ν (cm^{-1}): 3167.5 (N–H, amide), 3054.91 (C–H, aromatic), 2982.35 (C–H, aliphatic), 1724.34 (C=O, ketone), 1660.4 (C=O, amide).

General procedure for the synthesis of substituted 1,4-dihydropyridines (6a–d)

N-Aryl-3-oxobutanamide (***3a*** and ***3b***) (2 mmol), corresponding aldehyde (**4a–c**) (1 mmol) and ammonium acetate (**5**) (2 mmol) were all mixed and refluxed in 20 mL absolute ethanol for 24–48 h. The progress of the reaction was checked by TLC and on completion of the reaction; the product was filtered, washed with small portions of cold ethanol and then dried under vacuum to give the pure compounds **6a**–**d**. Physical and characteristic data of the final compounds are summarized in Table 1.

2,6-Dimethyl-3,5-bis-*N*-(2-benzothiazolyl) carbamoyl-4-(3-fluorophenyl)-1,4-dihydropyridine (6a)

Yellow precipitate; Yield 38%; ^{1}H NMR ($CDCl_3$): δ (ppm) 11.96 (2H, s, NH-amide), 9.05 (1H, s, NH-DHP), 6.91–7.98 (12H, m, ArH), 5.43 (1H, s, C4H-DHP), 2.30 (6H, s, CH_3-DHP); IR (KBr) ν (cm^{-1}): 3415.3 (N–H, DHP), 2913.2 (C–H, aliphatic), 1619.8 (C=O, amide), 1548.4 (C=C, alkene).

2,6-Dimethyl-3,5-bis-*N*-(2-benzothiazolyl) carbamoyl-4-(4-chlorophenyl)-1,4-dihydropyridine (6b)

Yellow precipitate; Yield 36%; ^{1}H NMR ($CDCl_3$): δ (ppm) 11.94 (2H, s, NH-amide), 9.05 (1H, brs, NH-DHP), 7.18–8.01 (12H, m, ArH), 5.40 (1H, s, C4H-DHP), 2.52 (6H, s, CH_3-DHP); IR (KBr) ν (cm^{-1}): 3397.5 (N–H, DHP), 2965.1 (C–H, aliphatic), 1623.3 (C=O, amide), 1592.7 (C=C, alkene).

2,6-Dimethyl-3,5-bis-*N*-(4-methyl-2-benzothiazolyl) carbamoyl-4-(3-bromophenyl)-1,4-dihydropyridine (6c)

Yellow precipitate; Yield 45%; ^{1}H NMR ($CDCl_3$): δ (ppm) 11.60 (2H, brs, NH-amide), 6.98–7.58 (10H, m, ArH), 5.86 (1H, s, NH-DHP), 5.19 (1H, s, C4H-DHP), 2.57 (6H, s, CH_3-DHP), 2.35 (6H, s, CH_3-benzathiazole); IR (KBr) ν (cm^{-1}): 3313.1 (N–H, DHP), 2923.2 (C–H, aliphatic), 1655.4 (C=O, amide), 1529 (C=C, alkene).

2,6-Dimethyl-3,5-bis-*N*-(4-methyl-2-benzothiazolyl) carbamoyl-4-(4-chlorophenyl)-1,4-dihydropyridine (6d)

Yellow precipitate; Yield 36%; ^{1}H NMR ($CDCl_3$): δ (ppm) 9.85 (2H, brs, NH-amide), 7.07–7.54 (10H, m, ArH), 6.04 (1H, brs, NH-DHP), 5.05 (1H, s, C4H-DHP), 2.52 (6H,

Table 1 Physical and analytical data of synthesized DHP compounds **6a–d**

Comp. code	Chemical structure	Mol. formula (mol. wt.)	Physical appearance	mp (°C)	Yield (%)
6a	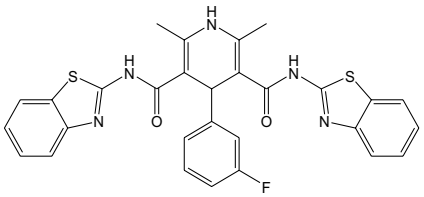	$C_{29}H_{22}FN_5O_2S$ (555.65)	Yellow	Decompose	38
6b	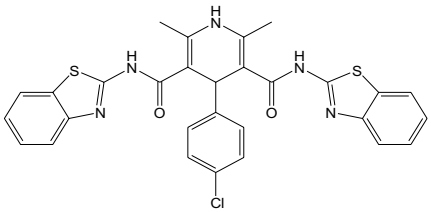	$C_{29}H_{22}ClN_5O_2S_2$ (572.1)	Yellow	Decompose	36
6c	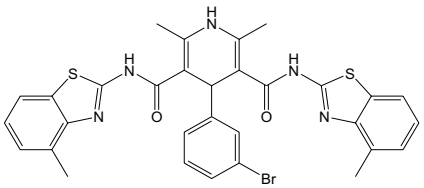	$C_{31}H_{26}BrN_5O_2S_2$ 644.6	Yellow	218–220	45
6d	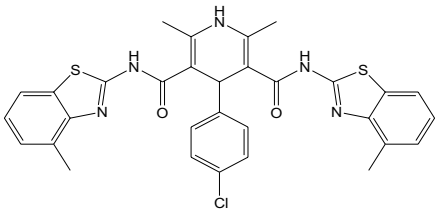	$C_{31}H_{26}ClN_5O_2S_2$ 600.15	Yellow	178–180	36

s, CH_3-DHP), 2.26 (6H, s, CH_3-benzathiazole); IR (KBr) ν (cm^{-1}): 3313.7 (N–H, DHP), 2921.2 (C–H, aliphatic), 1658.7 (C=O, amide), 1592.8 (C=C, alkene).

Biological assessment

Antibacterial activities of DHP derivatives (**6a**–**d**) were determined through a microdilution broth method according to CLSI protocol. In this method, the 96-well microplate was used and the stock solutions of each chemically synthesized compound were prepared. At the next step, various tested concentrations of compounds were prepared (1–512 µg/mL) and loaded into defined rows of 96-well microplates in sterile microplates 2–11. 100 µL sterile Mueller–Hinton broth was poured in sterile microplates 2–12 and after adding an appropriate amount of stock solution to microplates 2, using broth, the volume was brought to 200 µL. Twofold serial dilutions were carried out from microplates 2–11, and excess broth (100 µL) was discarded from the microplate 11. 100 µL of standard inoculums (1.5×10^8 CFU/mL) was added to microplates 2–12 in follow. The negative control rows for each case consisted of only culture media (Mueller–Hinton broth), without bacterial suspension (microplate 1). The positive control rows consisted of culture media (Mueller–Hinton broth) and the bacterial suspension (microplate 12). The positive control rows lacked a test compound. Ciprofloxacin was used as standard. MICs were recorded after incubating the inoculated microplates at 37 °C for 24 h.

Results and discussion

Crystal structures selected in this study (PDB ID **3FV5**) and (PDB ID **1SFJ**) are related to *E. coli* topoisomerase IV and *S. aureus* 3-dehydroquinate dehydratase, respectively. Topoisomerase IV is essential for unlinking or deactivating DNA following DNA replication. Topoisomerase IV is also responsible for relaxing positive supercoils. Topoisomerase IV is the target for quinolone-based antibacterial compounds that is able to overset the enzyme into a DNA damaging agent [22].

3-Dehydroquinate dehydratase is an enzyme which catalyzes the conversion of 3-dehydroquinate into 3-dehydroshikimate in the third step of the shikimate pathway [23]. The shikimate pathway, an essential pathway in many plants, bacteria and parasites [24], allows plants, fungi and bacteria for biosynthesis of aromatic amino acids [23], so has become important in development of herbicides and antimicrobial agents [24].

Docking validation

A docking method was validated by re-docking of the co-crystallographic ligands with the codes of DHK (**1SFJ**) and 1EU (**3FV5**). For the docked molecules, top-ranked binding modes of DHK and 1EU were compared with the original crystallographic poses (Table 2). On the basis of data, both of the selected targets could be used in this study since the RMSD values were found to be lower than 2 Å (0.61 and 1.18 for 3FV5 and 1SFJ, respectively).

Another important factor is the number of ligand conformations in the top-ranked cluster. As it is obvious from the data, all the top-ranked docking clusters were supported by high conformational populations. Moreover, top clusters showed good RMSDs with regard to crystallographic ligands. In the next step, AutoDock parameters that were used to validate the method (desired docking parameters in the software) could be applied to VS of chemical structures.

Table 2 AutoDock 4.2 validation results for bacterial holo PDB structures (3FV5 and 1SFJ)

PDB code	Resolution (Å)	GA runs	Maximum no. of energy evaluations	Population in the optimum cluster (out of 100)	RMSD from reference structure (Å)
3FV5	1.80	50	25×10^5	48	0.61
1SFJ	2.40	50	25×10^5	50	1.18

SBVS

Modern drug discovery techniques rely on the VS of chemical entities to identify hit/lead candidates [25]. Molecules with binding energies lower than − 8 kcal mol^{-1} were removed from the study. On the basis of this filtration, fifty molecules were selected. Obtained compounds (in silico candidates) were subjected to a multi-filtration protocol. The filtration criteria were chosen as conformational population of top-ranked cluster and interaction with key residues of the relevant targets.

To explain more, those binding energies that were supported with populated top-ranked clusters and superior binding interactions passed the filter. On the basis of this strategy, four molecules (**6a**–**d**) were picked up as

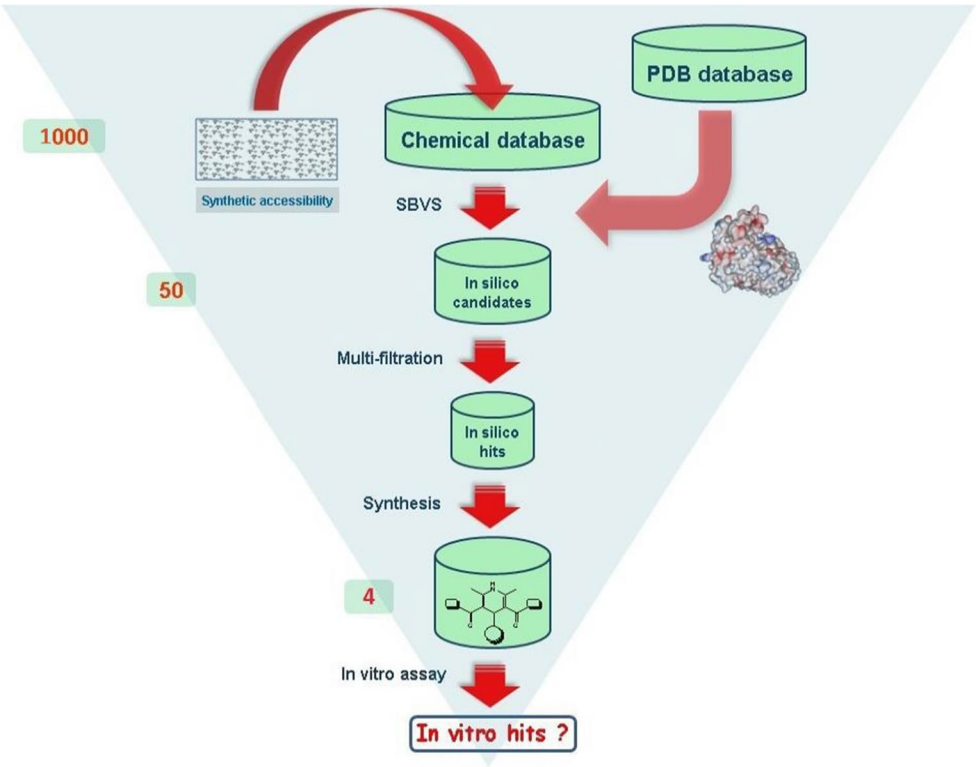

Fig. 1 Hierarchical view of the multi-step VS procedure to identify antibacterial DHPs

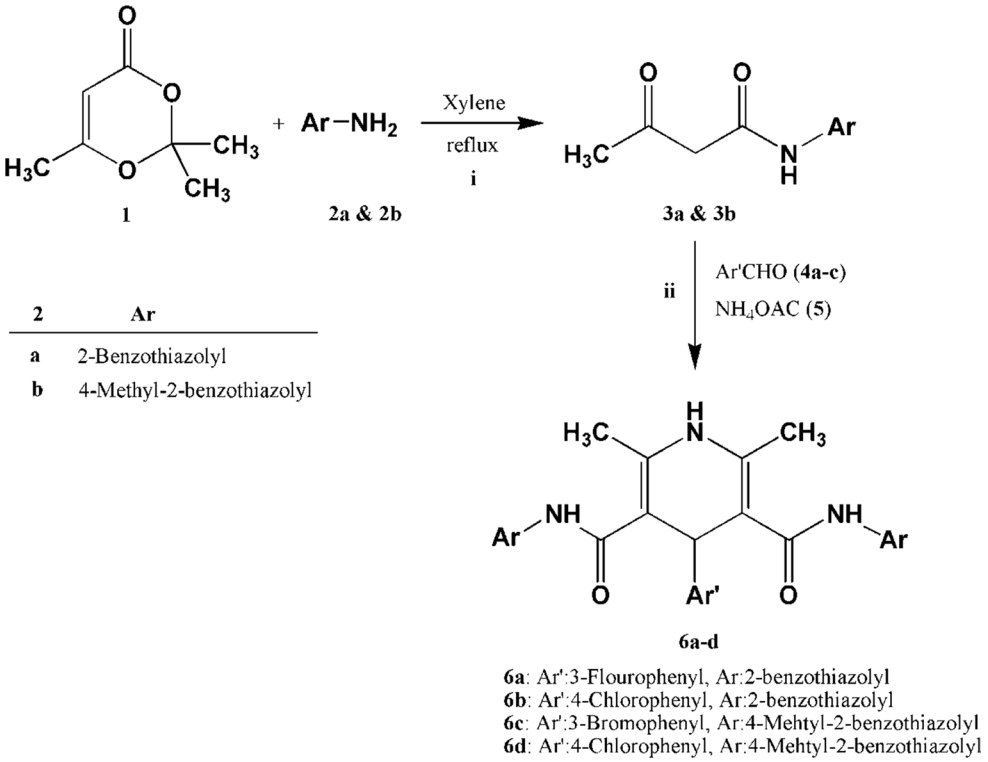

Scheme 1 Synthetic route to DHP derivatives: (i) xylene, reflux, 1–4 h; (ii) EtOH, reflux, 24–48 h

2	Ar
a	2-Benzothiazolyl
b	4-Methyl-2-benzothiazolyl

6a: Ar':3-Flourophenyl, Ar:2-benzothiazolyl
6b: Ar':4-Chlorophenyl, Ar:2-benzothiazolyl
6c: Ar':3-Bromophenyl, Ar:4-Mehtyl-2-benzothiazolyl
6d: Ar':4-Chlorophenyl, Ar:4-Mehtyl-2-benzothiazolyl

hit compounds for synthesis and antibacterial assessment (Fig. 1).

Chemistry

Selected DHP molecules (**6a**–**d**) were prepared through the synthetic route depicted in Scheme 1. Molecular condensation of *N*-aryl-acetoacetamides (**3a** and **3b**), aromatic aldehydes (**4a–c**) and ammonium acetate (**5**) in absolute ethanol afforded the desired 2,6-dimethyl-4-aryl/heteroaryl-*3,5*-bis-*N*-(aryl/heteroaryl) carbamoyl-1,4 dihydropyridines (**6a–d**) in fairly good yields (36–45%) (Table 1).

Biological evaluation

Compounds **6a**, **6b**, **6c** and **6d** were subjected to in vitro antibacterial activity assessment against *E. coli* and *S. aureus*. The utilized method was microdilution broth. Results are summarized in Table 3.

As shown in Table 3, screened DHP derivatives exhibited variable antibacterial activities against gram-positive bacteria *S. aureus* and gram-negative bacteria *E. coli*. In the whole series, the MIC (minimum inhibitory concentration) values of various tested chemical compounds ranged between 64 and 256 µg/mL against *S. aureus*. Compound **6d** displayed the highest antibacterial activity against *S. aureus* with MIC 64 µg/mL. The remaining compounds showed medium (**6c** 128 µg/mL) or weak antibacterial effects (**6a** and **6b** 256 µg/mL) against *S. aureus*. Compound **6c** was the only compound that exhibited antibacterial activity against *E. coli* (256 µg/mL).

Structure binding relationship of DHP derivatives

Binding residues of candidate targets (*E. coli* topoisomerase IV **3FV5** and *S. aureus* 3-dehydroquinate dehydratase **1SFJ**) are summarized in Table 4. Compound **6a** did not show any hydrogen bonds with the residues of topoisomerase IV. This feature was unique for compound **6a** since other candidate molecules exhibited H bonds in the active site of target. For more clarification, estimated binding energies of different ligand–enzyme complexes are also summarized in Table 4. The NH of the DHP ring participated in hydrogen bond interactions with oxygen atom of aspartate group in Asp45

Table 3 In vitro antibacterial activities of DHP compounds **6a–d** in microdilution method

Comp.	Minimum inhibitory concentration (µg/mL)	
	S. aureus	*E. coli*
6a	256	–
6b	256	–
6c	128	256
6d	64	–

Table 4 Interaction energies and H-bond/hydrophobic contact characteristics of virtual screened hits within *E. coli* topoisomerase IV (**3FV5**) and *S. aureus* 3-dehydroquinate dehydratase (**1SFJ**)

Comp.	Target	Estimated ΔG_b (kcal/mol)	No of H bonds	Involved amino acid	Involved atom of ligand	H-bond length (Å)	Involved residues (hydrophobic interaction)
6a	3FV5	− 8.65	0	–	–	–	Val165, Ser43, Val39, Asn42, Gln46, Pro75, Ile90, Arg93, Asp45, Met74, Thr163, Asp69, Val67
6b	3FV5	− 8.72	2	Arg72….NH_2 Asp45….OD2	O13 N6	2.96 3.04	His79, Asp77, Pro75, Arg132, Met74, Asp69, Glu46, Thr163, Gly73, Arg72, Ile78
6c	3FV5	− 10	1	Asn42….OD1	N6	3.51	Asp45, Asn42, Met74, Ile90, 72, Gly73, Ile90, Ala86, Leu89, Pro75, Thr163, Asn42, Glu136, Ala86,
6d	3FV5	− 8.22	2	Arg72….NH_2 Asp45….OD2	O13 N6	2.92 3.09	Met74, Leu89, Asn42, Ile90, Ile116, Arg93, Arg132, Glu46, Gly73, Thr163
6a	1SFJ	− 10.11	1	Tyr77….OH	N6	3.04	Pro220, Gly224, Phe135, Gln221, Pro223, Glu136, Lys72, Ala222
6b	1SFJ	− 10.23	3	Tyr77….OH Tyr77….OH Gly75….O	N20 N14 N25	2.88 2.97 3.26	Arg37, Lys72, Pro220, Ala222, Phe135, Thr11, Gln221, Pro223, Tyr77, Gly75
6c	1SFJ	− 10.30	3	Tyr77….OH Gln221….O Gly75….O	N6 N20 N14	2.79 2.57 3.14	Lys72, Tyr77, Gln221, Gly75, Thr9, Ala222, Gln225, Lys160, Arg37, His133, Arg70, Phe135, Pro223, Glu136, Leu73
6d	1SFJ	− 10.67	2	Glu136….OE2 Tyr77….OH	N20 N25	3.20 2.91	Gln221, Thr11, Arg37, Gly75, Lys72, Leu73, Asn134, His133, Glu136, Phe135, Tyr77, Pro223

(compounds **6b** and **6d**) and oxygen atom of amide carbonyl in the side chain of Asn42 (compound **6c**).

Interacted residues of topoisomerase showed that variation of substituents in the C3 and C5 of DHP ring might significantly change the binding pattern of candidate molecules. This could be obvious from the data of Table 4. Relatively different hydrophobic residues were found to make contacts with DHP scaffolds. Analysis of data indicated that Met74 and Thr163 interacted with all of the DHP structures and hence seemed important hydrophobic participants.

In the case of compound **6d**, two nitrogen atoms of benzothiazole ring participated in hydrogen bond interactions with Tyr77 and Glu136 residues of *S. aureus* 3-dehydroquinate dehydratase target (**1SFJ**). Tyr77 was involved in H-bond interaction with DHP nitrogen in compounds **6a** and **6c**. Compound **6d** made hydrophobic contact with Asn134 and such interaction could not be detected for other compounds under study. When comparing compounds **6b** (MIC 256 µg/mL) and **6c** (MIC 128 µg/mL), it was seen that both of the molecules made three hydrogen bonds with the active site of the target, while more hydrophobic residues were involved in binding to compound **6c**. Lower antibacterial effects of compounds **6a** and **6b** might be in accordance with less hydrophobic contacts through aromatic rings. Moreover, it was revealed that the halogen substituent of compound **6d** did not participate in any loose contacts.

Results of the present study might be further exploited. Candidate compounds against gram-negative bacteria must have an acceptable polarity, while such rationalization is not significant for gram-positive bacteria. As it was explained above, the most potent compound **6d** against *S. aureus* as gram-positive bacteria showed significant hydrophobic contacts in the active site if target.

Conclusion

A multi-step VS methodology, chemical synthesis and in vitro antibacterial assessment were applied to identify potential antibacterial scaffolds with 3,5-bis-*N*-aryl carbamoylated-4-aryl-1,4-dihydropyridine structure. Results showed that the most potent in vitro hit could potentiality inhibit the growth of gram-positive bacteria *S. aureus* (MIC 64 µg/mL). On the basis of obtained results, 4-methyl benzothiazole-3,5-bis-*N*-aryl carbamoylated-4-aryl-1,4-dihydropyridine structure may provide the opportunity to further development into more potent anti *S. aureus* agents. Results of such studies may be important since there is an urgent requirement to build up bioactive compounds that trigger several targets within a pathogen system.

Funding Funding was provided by Ferdowsi University of Mashhad (Grand No. Research Project No. 3/32040 - 1393/07/19).

References

1. M.L. Cohen, Nature **406**, 762 (2000)
2. H. Mahdavi, O. Rahmani, A.R. Shaverdi, J. Iran. Chem. Soc. **14**, 37 (2017)

3. S. Mandal, M. Moudgil, S.K. Mandal, Eur. J. Pharmacol. **625**, 90 (2009)
4. D. Horvath, J. Med. Chem. **40**, 2412 (1997)
5. Y. Biran, C.L. Masters, K.J. Barnham, A.I. Bush, P.A. Adlard, J. Cell Mol. Med. **13**, 61 (2009)
6. T. Tomašić, A. Kovač, G. Klebe, D. Blanot, S. Gobec, D. Kikelj, L.P. Mašič, J. Mol. Model **18**, 1063 (2012)
7. A. Srinivas Reddy, S. Priyadarshini Pati, P. Praveen Kumar, H.N. Pradeep, G. Narahari Sastry, Curr. Protein Pept. Sci. **8**, 329 (2007)
8. C.N. Cavasotto, Curr. Top. Med. Chem. **11**, 1528 (2011)
9. H. Azizian, F. Nabati, A. Sharifi, F. Siavoshi, M. Mahdavi, M. Amanlou, J. Mol. Model **18**, 2917 (2012)
10. P.J. Ballester, M. Mangold, N.I. Howard, R.L. Robinson, C. Abell, J. Blumberger, J.B. Mitchell, J.R. Soc, Interface **9**(77), 3196 (2012)
11. Z. Yu, L. Song, L. Tong, Y. Wang, W. Zheng, X. Gong, Wei Sheng Wu Xue Bao **56**(2), 219 (2016)
12. M. Katoh, M. Nakajima, H. Yamazaki, T. Yokoi, Pharm. Res. **17**(10), 1189 (2000)
13. I. Sabakhi, V. Topuzyan, Z. Hajimahdi, B. Daraei, H. Arefi, A. Zarghi, Des. IJPR **14**(4), 1087 (2015)
14. N.C. Desai, A.R. Trivedi, H.C. Somani, K.A. Bhatt, Chem. Biol. Drug Des. **86**, 370 (2015)
15. R. Surendra Kumar, A. Idhayadhulla, A. Jamal Abdul Nasser, S. Kavimani, S. Indumathy, Indian J. Pharm. Sci. **72**(6), 719 (2010)
16. N. Rao, K. Lakshimi, Sci. Rev. Chem. Commun. **3**(3), 141 (2013)
17. P.K. Mithlesh, P.K. Pareek, K. Ravikant, K.G. Ojha, Der. Pharma. Chem. **3**(2), 66 (2011)
18. T. Akbarzadeh, A. Fallah Tafti, N. Samadi, A. Foroumadi, M. Amanlou, M.A. Faramai, A. Shafiee, DARU **18**(2), 118 (2010)
19. G.M. Morris, R. Huey, W. Lindstrom, M.F. Sanner, R.K. Belew, D.S. Goodsell, A.J. Olson, J. Comput. Chem. **30**, 2785 (2009)
20. A.C. Wallace, R.A. Laskowski, J.M. Thornton, Protein Eng. **8**, 127 (1995)
21. R.J. Clemens, J.A. Hyatt, J. Org. Chem. **50**, 2431 (1985)
22. J. Kato, H. Suzuki, H. Ikeda, J. Biol. Chem. **267**, 25676 (1992)
23. K.M. Herrmann, Plant Physiol. **107**, 7 (1995)
24. K.M. Herrmann, Plant Cell **7**, 907 (1995)
25. J. Jiaranaikulwanitch, C. Boonyarat, V.V. Fokin, O. Vajragupta, Bioorg. Med. Chem. Lett. **20**, 6572 (2010)